NACA TN No. 1543

NATIONAL ADVISORY COMMITTEE FOR AERONAUTICS

TECHNICAL NOTE

No. 1543

EFFECT OF CHORDWISE LOCATION OF MAXIMUM THICKNESS ON THE SUPERSONIC WAVE DRAG OF SWEPTBACK WINGS

By Kenneth Margolis

Langley Memorial Aeronautical Laboratory
Langley Field, Va.

Washington
March 1948

NATIONAL ADVISORY COMMITTEE FOR AERONAUTICS

TECHNICAL NOTE NO. 1543

EFFECT OF CHORDWISE LOCATION OF MAXIMUM THICKNESS ON THE SUPERSONIC WAVE DRAG OF SWEPTBACK WINGS

By Kenneth Margolis

SUMMARY

On the basis of the linearized theory of supersonic flow, equations are derived for the wave drag of sweptback untapered wings at zero lift with thin double-wedge sections and arbitrary chordwise location of maximum thickness. Calculations are presented for a representative supersonic plan form.

The optimum location of maximum thickness for untapered supersonic wings is found to be at 50 percent chord, a symmetrical variation in wing wave-drag coefficient being exhibited about this minimum value. The drag variation is slight when considerable sweep behind the Mach lines is present and the variation is marked at Mach numbers where the wing approaches or is swept ahead of the Mach lines.

It is found that for tapered plan forms the sweep of the line of maximum thickness is an important sweep parameter insofar as drag due to thickness is concerned.

INTRODUCTION

A recent application (reference 1) of the linearized theory to the calculation of supersonic wave drag at zero lift of delta wings indicates that minimum drag for any double-wedge delta wing with sufficient sweep behind the Mach lines is obtained with location of maximum thickness at 10 to 20 percent chord. (In reference 1 and in the present paper the conventional definition of "delta plan forms" is modified to include those with sweptback trailing edges.) For a given delta plan form, a variation in maximum-thickness location necessarily implies a variation in the sweep of the line of maximum thickness and, therefore, no general predictions can be made for the drag effects induced by each parameter considered separately. In fact, there is evidence (see reference 2) to suggest that the sweep of the maximum-thickness line may be an important sweep parameter insofar as drag due to thickness is concerned. Hence, the problem of isolating the effects of chordwise location of maximum thickness immediately presents itself.

This problem is treated in the present paper by applying the method of reference 3 to derive the generalized wave-drag equations of sweptback untapered wings at zero lift having thin double-wedge sections with arbitrary maximum-thickness location. The wing tips are chosen parallel to the direction of flight and the range of supersonic Mach number for which the wing is swept ahead of and swept behind the Mach lines is considered. Typical distributions of section wave drag and wing wave-drag calculations are presented. Comparisons are made with two-dimensional theory and with results obtained for tapered wings.

SYMBOLS

x,y,z	Cartesian coordinates
V	velocity in flight direction
ρ	density of air
Δp	pressure increment
q	dynamic pressure $\left(\frac{1}{2}\rho V^2\right)$
φ	disturbance-velocity potential
M	Mach number
$\beta = \sqrt{M^2 - 1}$	
dz/dx	slope of airfoil surface
θ	half-wedge angle
c	chord length, measured in flight direction
h	location of maximum thickness, measured from leading edge
t	maximum thickness of section
Λ	angle of sweep, degrees
m	slope of leading edge $(\cot \Lambda)$
b	span of wing
$d = \frac{b/2}{m}$	
S	wing area

A	aspect ratio $\left(b^2/S\right)$
λ	taper ratio (ratio of tip chord to root chord)
c_{d_∞}	section wave-drag coefficient at spanwise station y exclusive of tip effect
$c_{d_{tip}}$	increment in section wave-drag coefficient at spanwise station y due to tip
c_d	section wave-drag coefficient at spanwise station y $\left(c_{d_\infty} + c_{d_{tip}}\right)$
C_{D_∞}	wing wave-drag coefficient exclusive of tip effect
$C_{D_{tip}}$	increment in wing wave-drag coefficient due to tip
C_D	wing wave-drag coefficient $\left(C_{D_\infty} + C_{D_{tip}}\right)$

ANALYSIS

The analysis is essentially that used in references 2 and 3. For convenience, a brief outline of the basic equations is presented.

The assumptions of small disturbances and a constancy of sonic velocity throughout the fluid lead to the linearized equation for the velocity potential φ

$$\left(1 - M^2\right)\varphi_{xx} + \varphi_{yy} + \varphi_{zz} = 0 \qquad (1)$$

where M is the Mach number of the flow and the derivatives are taken with respect to the variables x, y, and z of the Cartesian coordinate system. On the basis of this linear theory, a solution for a uniform sweptback line of sources in the pressure field is derived in reference 3. The pressure field associated with this solution corresponds to that over a semi-infinite sweptback airfoil of wedge section. The pressure coefficient $\Delta p/q$ at a spanwise station y and point x along the wedge for $m\beta \leq 1$ is

$$\frac{\Delta p}{q} = \frac{2}{\pi} \tan\theta \frac{m}{\sqrt{1 - m^2\beta^2}} \cosh^{-1} \frac{x - m\beta^2 y}{\beta|y - mx|} \qquad (2a)$$

and for $m\beta > 1$

$$\frac{\Delta p}{q} = \frac{2}{\pi} \tan \theta \frac{m}{\sqrt{m^2\beta^2 - 1}} \cos^{-1} \frac{x - m\beta^2 y}{\beta |y - mx|} \tag{2b}$$

where m is the slope of the leading edge of the wing, θ is the half-wedge angle ($\tan \theta \approx \theta$ since the angle is small), $\beta = \sqrt{M^2 - 1}$, and the origin of the line source is taken at (0,0). In the region between the leading edge and the Mach cone (that is, $\frac{1}{\beta} x \leq y \leq mx$), the real part of $\cos^{-1} \frac{x - m\beta^2 y}{\beta |y - mx|}$ is constant and equal to π.

Equation (2b) then reduces to

$$\frac{\Delta p}{q} = 2 \tan \theta \frac{m}{\sqrt{m^2\beta^2 - 1}} \tag{2c}$$

The distribution of pressure over sweptback wings of desired plan form and profile is obtained by appropriate superposition of wedge-type solutions. In order to satisfy the boundary condition over the surface of an untapered wing of double-wedge section, semi-infinite line sources are placed at the leading and trailing edge of the wing and a semi-infinite line sink is placed along the line of maximum thickness. The strengths of these lines are proportional to the wedge angles; therefore, in superimposing solutions of the type given in equations (2), the appropriate θ for each line source and sink must be found. The correct wedge angles necessary to obtain a double-wedge section of length c, maximum thickness t, and location of maximum thickness h are (see fig. 1)

$$\left.\begin{aligned} \theta_{\substack{\text{Leading}\\ \text{line source}}} &= \frac{c}{2h}\left(\frac{t}{c}\right) \\ \theta_{\substack{\text{Trailing}\\ \text{line source}}} &= \frac{c}{2(c-h)}\left(\frac{t}{c}\right) \\ \theta_{\text{Line sink}} &= \frac{c^2}{2h(c-h)}\left(\frac{t}{c}\right) \end{aligned}\right\} \qquad (3)$$

(It is convenient to express the angles in terms of the section thickness ratio $\frac{t}{c}$ as can be seen by reference to the drag integrals.) At the tip where the wing is cut off in the flight direction, reversed distributions of these sinks and sources are placed so as to cancel exactly the effects of the original distribution farther spanwise than the tip. Figure 1 shows the distributions of sinks and sources for an untapered wing of double-wedge section and identifies the system of axes and symbols associated with the derivation of the drag equations.

The disturbances caused by the elementary line sources and sinks are limited to the regions enclosed by their Mach cones; the Mach line configuration is presented in figure 2. For purposes of simplification the wings considered were restricted to those with no tip effects other than the effects each tip exerts on its own half of the wing.

The pressure coefficients obtained from superposition of solutions given in equations (2) are converted into drag coefficients by the following relations:

$$C_D = \frac{2}{S}\int_0^{b/2} c_d c \, dy = \frac{4}{S}\int_0^{b/2}\int_{L.E}^{T.E} \frac{\Delta p}{q}\frac{dz}{dx}\, dx\, dy \qquad (4)$$

where b is the wing span; S is the wing area; dz/dx is the slope of the airfoil surface; and L.E. and T.E. denote leading edge and trailing edge, respectively.

DERIVATION OF GENERALIZED EQUATIONS

The drag equations are derived for half of the wing since the drag is distributed symmetrically over both halves. The induced effects of the opposite half-wing are represented by the conjugate terms in the

integrands of the drag integrals. (The conjugate terms are obtained by considering the symmetrical arrangement of line sources and line sinks below the x-axis.)

For a double-wedge profile, $\frac{dz}{dx} = \frac{c}{2h}\left(\frac{t}{c}\right)$ from the leading edge to the maximum-thickness location and $\frac{dz}{dx} = -\frac{c}{2(c-h)}\left(\frac{t}{c}\right)$ from the maximum-thickness location to the trailing edge. The generalized equations, exclusive of tip effects, are obtained as follows: (See fig. 3 for information pertinent to integration limits.)

For $m\beta \leq 1$,

$$\frac{\pi S\sqrt{1-m^2\beta^2}}{8m(t/c)^2}C_{D_\infty} = \frac{\pi\sqrt{1-m^2\beta^2}}{4m(t/c)^2}\int_0^{b/2} c_{d_\infty} c\, dy$$

$$= \frac{c^2}{4h^2}\int_0^{md}\int_{y/m}^{\frac{y+mh}{m}} A\, dx\, dy - \frac{c^2}{4h(c-h)}\int_0^{md}\int_{\frac{y+mh}{m}}^{\frac{y+mc}{m}} A\, dx\, dy - \frac{c^3}{4h^2(c-h)}\left(\int_0^{\frac{mh}{1-m\beta}}\int_{y\beta+h}^{\frac{y+mh}{m}} B\, dx\, dy\right.$$

$$\left. + \int_{\frac{mh}{1-m\beta}}^{md}\int_{y/m}^{\frac{y+mh}{m}} B\, dx\, dy\right) + \frac{c^3}{4h(c-h)^2}\int_0^{md}\int_{\frac{y+mh}{m}}^{\frac{y+mc}{m}} B\, dx\, dy - \frac{c^2}{4(c-h)^2}\left[\int_0^{\frac{m(c-h)}{1-m\beta}}\int_{y\beta+c}^{\frac{y+mc}{m}} C\, dx\, dy\right.$$

$$\left. + \int_{\frac{m(c-h)}{1-m\beta}}^{md}\int_{\frac{y+mh}{m}}^{\frac{y+mc}{m}} C\, dx\, dy\right] + \frac{c^2}{4h(c-h)}\left[\int_{\frac{m(c-h)}{1-m\beta}}^{\frac{mc}{1-m\beta}}\int_{y\beta+c}^{\frac{y+mh}{m}} C\, dx\, dy + \int_{\frac{mc}{1-m\beta}}^{md}\int_{y/m}^{\frac{y+mh}{m}} C\, dx\, dy\right] \qquad (5a)$$

where A, B, and C, which refer to the pressures resulting from the leading line sources, line sinks, and trailing line sources, respectively, are as follows:

$$A = \cosh^{-1}\frac{x - m\beta^2 y}{\beta|y - mx|} + \cosh^{-1}\frac{x + m\beta^2 y}{\beta|y + mx|}$$

$$B = \cosh^{-1}\frac{x - h - m\beta^2 y}{\beta|y - m(x - h)|} + \cosh^{-1}\frac{x - h + m\beta^2 y}{\beta|y + m(x - h)|}$$

$$C = \cosh^{-1}\frac{x - c - m\beta^2 y}{\beta|y - m(x - c)|} + \cosh^{-1}\frac{x - c + m\beta^2 y}{\beta|y + m(x - c)|}$$

For $m\beta > 1$,

$$\frac{\pi S\sqrt{m^2\beta^2 - 1}}{8m(t/c)^2} C_{D_\infty} = \frac{\pi\sqrt{m^2\beta^2 - 1}}{4m(t/c)^2}\int_0^{b/2} c_{d_\infty} c\, dy$$

$$= \frac{c^2\pi}{4h^2}\left(\int_0^{\frac{mh}{m\beta-1}}\int_{y/m}^{y\beta} dx\, dy + \int_{\frac{mh}{m\beta-1}}^{md}\int_{y/m}^{\frac{y+mh}{m}} dx\, dy\right) - \frac{c^2\pi}{4h(c-h)}\left(\int_{\frac{mh}{m\beta-1}}^{\frac{mc}{m\beta-1}}\int_{\frac{y+mh}{m}}^{y\beta} dx\, dy\right.$$

$$\left. + \int_{\frac{mc}{m\beta-1}}^{md}\int_{\frac{y+mh}{m}}^{\frac{y+mc}{m}} dx\, dy\right) + \frac{c^3\pi}{4h(c-h)^2}\left[\int_0^{\frac{m(c-h)}{m\beta-1}}\int_{\frac{y+mh}{m}}^{y\beta+h} dx\, dy + \int_{\frac{m(c-h)}{m\beta-1}}^{md}\int_{\frac{y+mh}{m}}^{\frac{y+mc}{m}} dx\, dy\right]$$

$$+ \frac{c^2}{4h^2}\int_0^{\frac{mh}{m\beta-1}}\int_{y\beta}^{\frac{y+mh}{m}} D\, dx\, dy - \frac{c^2}{4h(c-h)}\left(\int_{\frac{mh}{m\beta-1}}^{\frac{mc}{m\beta-1}}\int_{y\beta}^{\frac{y+mc}{m}} D\, dx\, dy\right.$$

$$\left. + \int_0^{\frac{mh}{m\beta-1}}\int_{\frac{y+mh}{m}}^{\frac{y+mc}{m}} D\, dx\, dy\right) + \frac{c^3}{4h(c-h)^2}\int_0^{\frac{m(c-h)}{m\beta-1}}\int_{y\beta+h}^{\frac{y+mc}{m}} E\, dx\, dy \qquad (5b)$$

where D and E, which refer to the pressures resulting from the leading line sources and from the line sinks, respectively, are as follows:

$$D = \cos^{-1} \frac{x - m\beta^2 y}{\beta|y - mx|} + \cos^{-1} \frac{x + m\beta^2 y}{\beta|y + mx|}$$

$$E = \cos^{-1} \frac{x - h - m\beta^2 y}{\beta|y - m(x - h)|} + \cos^{-1} \frac{x - h + m\beta^2 y}{\beta|y + m(x - h)|}$$

It should be noted that equations (5) give the drag for plan forms where the tip is placed farther spanwise than the points of intersection between the Mach lines and the leading and the trailing edges (see fig. 3). Deletion of certain integrals and appropriate changes in the y-limits of other integrals may be made for configurations where the tip is placed nearer the root chord. Equations (5) are evaluated and the resulting section wave-drag and wing wave-drag formulas for all untapered plan forms are presented in appendix A.

It was stated previously that the wings considered have no tip effects other than those each tip exerts on its own half of the wing; that is, the Mach lines from one tip do not enclose any part of the opposite half-wing. This condition is expressed mathematically as follows:

For $m\beta \leq 1$, the aspect ratio

$$A \geq \frac{1}{\beta} \tag{6a}$$

and for $m\beta > 1$, the aspect ratio

$$A \geq \frac{2m}{m\beta + 1} \tag{6b}$$

The wave-drag contribution of the tip for $m\beta \leq 1$ is (see fig. 3)

$$\frac{\pi S\sqrt{1-m^2\beta^2}}{8m(t/c)^2}C_{D_{tip}} = \frac{\pi\sqrt{1-m^2\beta^2}}{4m(t/c)^2}\int_{\frac{md(1+m\beta)-mc}{1+m\beta}}^{b/2} c_{d_{tip}}\, c\, dy$$

$$= -\frac{c^2}{4h^2}\int_{\frac{md(1+m\beta)-mh}{1+m\beta}}^{md}\int_{d(1+m\beta)-y\beta}^{\frac{y+mh}{m}} F\, dx\, dy$$

$$+\frac{c^2}{4h(c-h)}\left[\int_{\frac{md(1+m\beta)-mc}{1+m\beta}}^{\frac{md(1+m\beta)-mh}{1+m\beta}}\int_{d(1+m\beta)-y\beta}^{\frac{y+mc}{m}} F\, dx\, dy\right.$$

$$\left.+\int_{\frac{md(1+m\beta)-mh}{1+m\beta}}^{md}\int_{\frac{y+mh}{m}}^{\frac{y+mc}{m}} F\, dx\, dy\right]$$

$$-\frac{c^3}{4h(c-h)^2}\int_{\frac{md(1+m\beta)-m(c-h)}{1+m\beta}}^{md}\int_{d(1+m\beta)+h-y\beta}^{\frac{y+mc}{m}} G\, dx\, dy \qquad (7)$$

where F and G, which refer to the pressures resulting from the leading line sink and from the line source, respectively, are as follows:

$$F = \cosh^{-1}\frac{x-d-m\beta^2(y-md)}{\beta|y-mx|}$$

$$G = \cosh^{-1}\frac{x-d-h-m\beta^2(y-md)}{\beta|y-m(x-h)|}$$

For $m\beta > 1$, equation (7) is still valid if $\sqrt{1-m^2\beta^2}$ is changed to $\sqrt{m^2\beta^2-1}$ and the inverse hyperbolic function $\cosh^{-1}$ is changed to the inverse cosine function $\cos^{-1}$.

Equation (7) is evaluated and the results presented in appendix B. The total wave-drag coefficients are then obtained by the following relations:

$$\left.\begin{aligned} c_d &= c_{d_\infty} + c_{d_{tip}} \\ C_D &= C_{D_\infty} + C_{D_{tip}} \end{aligned}\right\} \qquad (8)$$

It is found that $C_{D_{tip}}$ is identically equal to zero and, hence, $C_D = C_{D_\infty}$ for wings satisfying the aspect-ratio limitations imposed in equations (6).

When the expression for C_D is differentiated with respect to h in order to find an optimum maximum-thickness location, it is found that

$$\left(\frac{\partial C_D}{\partial h}\right)_{h=\frac{c}{2}} \equiv 0 \qquad (9)$$

and that the drag function is minimized at this value of h independently of the other parameters. It is also seen from the drag equations that the distributions are symmetrical about this minimum point.

RESULTS AND DISCUSSION

For calculation purposes, an untapered plan form of aspect ratio 2 and sweepback of 60° has been used. Equation (9) indicates that the trends obtained for this representative plan form are equally valid for all untapered wings with double-wedge profiles. The results may be assumed to have qualitative application to curved profiles without cusps.

Section wave drag.- Spanwise distributions of section wave-drag coefficient are shown in figures 4 and 5 for Mach numbers of 1.414 and 3, respectively. At a Mach number of 1.414 the wing is swept behind the Mach lines, and at a Mach number of 3 the wing is swept ahead of the Mach lines. In each figure maximum-thickness locations are varied from 20 percent chord to 80 percent chord. Variations in maximum-thickness location need actually only be considered up to 50 percent chord; the results for any arbitrary percent chord k and $(100 - k)$ are equal because of symmetry considerations. (See drag equations in appendix A.) When the wing is swept behind the Mach lines (fig. 4), the centroid of the drag forces on a wing panel moves noticeably inboard with forward

or rearward shift of the maximum thickness from the midpoint position. When the wing is swept ahead of the Mach lines (fig. 5), little change is noted in the centroid.

Wing wave drag.- Variation of wing wave-drag coefficient with Mach number is shown in figure 6. As was mentioned previously in the mathematical discussion of the drag equations, the symmetrical section is seen to be the optimum profile for an untapered plan form insofar as minimum drag is concerned. The variation of wing wave-drag coefficient with maximum-thickness location does not appear to be too significant when the wing is swept far behind the Mach lines; however, as the "critical" condition is approached (that is, $m\beta = 1$) the variation becomes more noticeable. There is seen to be a marked drag variation with maximum-thickness location in this region and for Mach numbers where the wing is swept ahead of the Mach lines.

Figure 7 is, in effect, a cross plot of figure 6 and presents variation of wing wave-drag coefficient with maximum-thickness location for Mach numbers of 1.414 and 3. The previous remarks are clearly illustrated in this figure by the flat curve at the lower Mach number and by the curve with a well-defined minimum at the higher Mach number.

Comparison with two-dimensional theory.- If m approaches infinity (that is, a rectangular plan form), the drag equation reduces to

$$\frac{C_D}{(t/c)^2} = \frac{1}{\sqrt{M^2 - 1}} \frac{c^2}{h(c - h)} \qquad (10)$$

which is exactly the result obtained by Ackeret for two-dimensional flow (see reference 4). This result is expected since the plan forms considered have zero increment in wing wave drag due to the wing tip. The two-dimensional (Ackeret solution) and three-dimensional (swept-back wing) results, therefore, exhibit the same qualitative drag effects due to variation in maximum-thickness location - that is, a drag variation symmetrical about a minimum value at 50 percent chord. Of course the quantitative results are quite different, the three-dimensional value being lower when considerable sweep behind the Mach lines is present and the two-dimensional value being less for other conditions. Figure 8 presents the variation of two-dimensional drag with Mach number for different maximum-thickness locations. Comparison with the three-dimensional result for the wing of aspect ratio 2 and sweepback of 60° is also indicated in this figure.

Comparison with tapered wings.- The results presented in reference 1 for a given delta plan form ($\lambda = 0$) indicate an optimum maximum-thickness location at 10 to 20 percent chord when the wing is swept sufficiently behind the Mach lines. The results obtained in the present

investigation for untapered wings ($\lambda = 1$) indicate an optimum maximum-thickness location at 50 percent chord. Hence, the optimum location for any arbitrary and conventional tapered wing ($0 \leqq \lambda \leqq 1$) with sufficient sweep behind the Mach lines approaches the 10-percent to 20-percent value for small taper ratios (large taper) and the 50-percent value for large taper ratios (small taper).

For a given delta plan form, the sweep of the maximum-thickness line varies with the location of maximum thickness and thus no prediction can be made for the drag effects induced by each parameter considered separately. For an untapered wing, however, the effects of maximum-thickness location are isolated since the sweep of the maximum-thickness line remains constant. Inasmuch as the present results indicate an adverse drag effect due to shifting the maximum-thickness location forward of the 50-percent location, the optimum location of maximum thickness for the delta wings of reference 1 of between 10 and 20 percent chord must result from the increased sweep of the line of maximum thickness at the forward location. The sweep of the line of maximum thickness thus appears to be an important sweep parameter for tapered wings insofar as drag due to thickness is concerned. This inference is further supported in reference 2 in which the section wave-drag coefficient at the root of tapered wings is found to be a function of the Mach number and the sweep of the maximum-thickness line and is found to be independent of leading-edge and trailing-edge sweep.

CONCLUSIONS

The following conclusions refer specifically to nonlifting wings with double-wedge profiles but may be assumed to have application to curved supersonic profiles without cusps:

1. The optimum location of maximum thickness for untapered supersonic wings is at 50 percent chord, a symmetrical variation in wing wave-drag coefficient being exhibited about this minimum value similar to that found in two-dimensional supersonic flow.

2. The variation of wing wave-drag coefficient with maximum-thickness location is slight when the wing is swept far behind the Mach lines and is marked at Mach numbers where the wing approaches or is swept ahead of the Mach lines.

3. The sweep of the line of maximum thickness is an important sweep parameter for tapered wings insofar as drag due to thickness is concerned.

Langley Memorial Aeronautical Laboratory
National Advisory Committee for Aeronautics
Langley Field, Va., October 31, 1947

APPENDIX A

EVALUATION OF EQUATIONS (5) FOR SECTION WAVE DRAG AND WING WAVE DRAG EXCLUSIVE OF TIP EFFECTS $\left(*\frac{h}{c} \leq 0.5\right)$

Section Drag for $m\beta \leq 1$

$$\frac{c\pi\sqrt{1 - m^2\beta^2}}{4m(t/c)^2} c_{d_\infty} = A \qquad \text{for} \qquad 0 \leq y \leq \frac{mh}{1 - m\beta}$$

$$= A + B \qquad \frac{mh}{1 - m\beta} < y \leq \frac{m(c - h)}{1 - m\beta}$$

$$= A + B + C \qquad \frac{m(c - h)}{1 - m\beta} < y \leq \frac{mc}{1 - m\beta}$$

$$= A + B + C + D \qquad \frac{mc}{1 - m\beta} < y < \infty$$

where

$$A = \frac{c^3}{4h^2(c - h)}\left[\frac{2y + mh}{m}\cosh^{-1}\frac{y(1 + m^2\beta^2) + mh}{m\beta(2y + mh)} + h\cosh^{-1}\frac{y(1 - m^2\beta^2) + mh}{m^2h\beta}\right]$$

$$+ \frac{c^3}{4h(c - h)^2}\left\{\frac{2y + m(c - h)}{m}\cosh^{-1}\frac{y(1 + m^2\beta^2) + m(c - h)}{m\beta\left[2y + m(c - h)\right]}\right.$$

$$\left. + (c - h)\cosh^{-1}\frac{y(1 - m^2\beta^2) + m(c - h)}{m^2(c - h)\beta}\right\}$$

$$- \frac{c^2}{4h(c - h)}\left[\frac{2y + mc}{m}\cosh^{-1}\frac{y(1 + m^2\beta^2) + mc}{m\beta(2y + mc)} + c\cosh^{-1}\frac{y(1 - m^2\beta^2) + mc}{m^2c\beta}\right]$$

$$- \frac{c^2(c^2 - ch + h^2)}{h^2(c - h)^2}\frac{y}{m}\cosh^{-1}\frac{1 + m^2\beta^2}{2m\beta}$$

---

*The equations are symmetrical about the point $\frac{h}{c} = 0.5$; for $\frac{h}{c} > 0.5$, use the same formulas and perform calculations for $\left(\frac{h}{c}\right)_{new} = 1 - \frac{h}{c}$

$$B = \frac{c^3}{4h^2(c-h)}\left[\frac{2y-mh}{m}\cosh^{-1}\frac{y(1+m^2\beta^2)-mh}{m\beta(2y-mh)} - h\cosh^{-1}\frac{y(1-m^2\beta^2)-mh}{m^2h\beta}\right]$$

$$C = \frac{c^3}{4h(c-h)^2}\left\{\frac{2y-m(c-h)}{m}\cosh^{-1}\frac{y(1+m^2\beta^2)-m(c-h)}{m\beta\left[2y-m(c-h)\right]}\right.$$

$$\left. - (c-h)\cosh^{-1}\frac{y(1-m^2\beta^2)-m(c-h)}{m^2(c-h)\beta}\right\}$$

and

$$D = \frac{-c^2}{4h(c-h)}\left[\frac{2y-mc}{m}\cosh^{-1}\frac{y(1+m^2\beta^2)-mc}{m\beta(2y-mc)} - c\cosh^{-1}\frac{y(1-m^2\beta^2)-mc}{m^2c\beta}\right]$$

Section Drag for $m\beta > 1$

$$\frac{c\pi\sqrt{m^2\beta^2-1}}{4m(t/c)^2}c_{d_\infty} = A + B + C \qquad \text{for} \qquad 0 \leq y \leq \frac{mh}{m\beta-1}$$

$$= B + C + D \qquad \frac{mh}{m\beta-1} < y \leq \frac{m(c-h)}{m\beta-1}$$

$$= C + 2D \qquad \frac{m(c-h)}{m\beta-1} < y \leq \frac{mc}{m\beta-1}$$

$$= D \qquad \frac{mc}{m\beta-1} < y < \infty$$

where

$$A = \frac{c^3}{4h^2(c-h)}\left[\frac{2y+mh}{m}\cos^{-1}\frac{y(1+m^2\beta^2)+mh}{m\beta(2y+mh)} + h\cos^{-1}\frac{y(1-m^2\beta^2)+mh}{m^2h\beta}\right]$$

$$B = \frac{c^3}{4h(c-h)^2}\left\{\frac{2y+m(c-h)}{m}\cos^{-1}\frac{y(1+m^2\beta^2)+m(c-h)}{m\beta\left[2y+m(c-h)\right]}\right.$$

$$\left. + (c-h)\cos^{-1}\frac{y(1-m^2\beta^2)+m(c-h)}{m^2(c-h)\beta}\right\}$$

$$C = \frac{-c^2}{4h(c-h)}\left[\frac{2y+mc}{m}\cos^{-1}\frac{y(1+m^2\beta^2)+mc}{m\beta(2y+mc)} + c\cos^{-1}\frac{y(1-m^2\beta^2)+mc}{m^2c\beta}\right]$$

and

$$D = \frac{c^3\pi}{4h(c-h)}$$

Wing Drag for $m\beta < 1$

$$\frac{\pi S\sqrt{1-m^2\beta^2}}{8m(t/c)^2}C_{D_\infty} = A \qquad \text{for} \qquad 0 < md \leq \frac{mh}{1-m\beta}$$

$$= A + B \qquad \frac{mh}{1-m\beta} < md \leq \frac{m(c-h)}{1-m\beta}$$

$$= A + B + C \qquad \frac{m(c-h)}{1-m\beta} < md \leq \frac{mc}{1-m\beta}$$

$$= A + B + C + D \qquad \frac{mc}{1-m\beta} < md < \infty$$

where

$$A = \frac{mc^3}{16h(c-h)}\left\{\frac{4d(1-m^2\beta^2)+h(3-m^2\beta^2)}{1-m^2\beta^2}\cosh^{-1}\frac{d(1-m^2\beta^2)+h}{mh\beta}\right.$$

$$+\frac{(2d+h)^2}{h}\cosh^{-1}\frac{d(1+m^2\beta^2)+h}{m\beta(2d+h)}$$

$$+\frac{[2d+(c-h)]^2}{c-h}\cosh^{-1}\frac{d(1+m^2\beta^2)+c-h}{m\beta(2d+c-h)}$$

$$+\frac{4d(1-m^2\beta^2)+(c-h)(3-m^2\beta^2)}{1-m^2\beta^2}\cosh^{-1}\frac{d(1-m^2\beta^2)+c-h}{m(c-h)\beta}$$

$$-\frac{4d(1-m^2\beta^2)+c(3-m^2\beta^2)}{1-m^2\beta^2}\cosh^{-1}\frac{d(1-m^2\beta^2)+c}{mc\beta}$$

$$-\frac{(2d+c)^2}{c}\cosh^{-1}\frac{d(1+m^2\beta^2)+c}{m\beta(2d+c)}$$

$$-\frac{8d^2(c^2-ch+h^2)}{(c-h)ch}\cosh^{-1}\frac{1+m^2\beta^2}{2m\beta}$$

$$+\frac{2}{\sqrt{1-m^2\beta^2}}\left[\sqrt{d^2(1-m^2\beta^2)+2cd+c^2}\right.$$

$$\left.\left.-\sqrt{d^2(1-m^2\beta^2)+2dh+h^2}-\sqrt{d^2(1-m^2\beta^2)+2d(c-h)+(c-h)^2}\right]\right\}$$

$$B = \frac{mc^3}{16h(c-h)}\left[\frac{(2d-h)^2}{h}\cosh^{-1}\frac{d(1+m^2\beta^2)-h}{m\beta(2d-h)}\right.$$

$$+\frac{2\sqrt{d^2(1-m^2\beta^2)-2dh+h^2}}{\sqrt{1-m^2\beta^2}}$$

$$\left.-\frac{4d(1-m^2\beta^2)-h(3-m^2\beta^2)}{1-m^2\beta^2}\cosh^{-1}\frac{d(1-m^2\beta^2)-h}{mh\beta}\right]$$

$$C = \frac{mc^3}{16h(c-h)}\left[\frac{(2d+h-c)^2}{c-h}\cosh^{-1}\frac{d(1+m^2\beta^2)-(c-h)}{m\beta(2d+h-c)}\right.$$

$$+\frac{2\sqrt{d^2(1-m^2\beta^2)-2d(c-h)+(c-h)^2}}{\sqrt{1-m^2\beta^2}}$$

$$\left.-\frac{4d(1-m^2\beta^2)-(c-h)(3-m^2\beta^2)}{1-m^2\beta^2}\cosh^{-1}\frac{d(1-m^2\beta^2)-(c-h)}{m(c-h)\beta}\right]$$

and

$$D = \frac{mc^3}{16h(c-h)}\left[\frac{4d(1-m^2\beta^2)-c(3-m^2\beta^2)}{1-m^2\beta^2}\cosh^{-1}\frac{d(1-m^2\beta^2)-c}{mc\beta}\right.$$

$$\left.-\frac{(2d-c)^2}{c}\cosh^{-1}\frac{d(1+m^2\beta^2)-c}{m\beta(2d-c)}-\frac{2\sqrt{d^2(1-m^2\beta^2)-2cd+c^2}}{\sqrt{1-m^2\beta^2}}\right]$$

Wing Drag for $m\beta > 1$

$$\frac{\pi S\sqrt{m^2\beta^2-1}}{8m(t/c)^2}C_{D_\infty} = A + B + C \qquad \text{for} \qquad 0 < md \leq \frac{mh}{m\beta-1}$$

$$= B + C \qquad \frac{mh}{m\beta-1} < md \leq \frac{m(c-h)}{m\beta-1}$$

$$= C \qquad \frac{m(c-h)}{m\beta-1} < md \leq \frac{mc}{m\beta-1}$$

$$= D \qquad \frac{mc}{m\beta-1} < md < \infty$$

where

$$A = \frac{mc^3}{16h(c-h)}\left\{\frac{h(m^2\beta^2-3)+4d(m^2\beta^2-1)}{m^2\beta^2-1}\cos^{-1}\frac{d(1-m^2\beta^2)+h}{mh\beta}\right.$$

$$+\frac{(2d+h)^2}{h}\cos^{-1}\frac{d(1+m^2\beta^2)+h}{m\beta(2d+h)}+\frac{2\sqrt{d^2(1-m^2\beta^2)+2hd+h^2}}{\sqrt{m^2\beta^2-1}}$$

$$\left.-\frac{\pi\left[h(m^2\beta^2-3)+4d(m^2\beta^2-1)\right]}{m^2\beta^2-1}\right\}$$

$$B = \frac{mc^3}{16h(c-h)}\left\{\frac{(2d+c-h)^2}{c-h}\cos^{-1}\frac{d(1+m^2\beta^2)+c-h}{m\beta(2d+c-h)}\right.$$

$$+\frac{2\sqrt{d^2(1-m^2\beta^2)+2d(c-h)+(c-h)^2}}{\sqrt{m^2\beta^2-1}}$$

$$+\frac{(c-h)(m^2\beta^2-3)+4d(m^2\beta^2-1)}{m^2\beta^2-1}\cos^{-1}\frac{d(1-m^2\beta^2)+c-h}{m\beta(c-h)}$$

$$\left.+\frac{\pi\left[(m^2\beta^2-3)(h-c)-4d(m^2\beta^2-1)\right]}{m^2\beta^2-1}\right\}$$

$$C = \frac{mc^3}{16h(c-h)}\left\{\frac{\pi\left[8d(m^2\beta^2-1)+c(m^2\beta^2-3)\right]}{m^2\beta^2-1}\right.$$

$$-\frac{2\sqrt{d^2(1-m^2\beta^2)+2cd+c^2}}{\sqrt{m^2\beta^2-1}}-\frac{(2d+c)^2}{c}\cos^{-1}\frac{d(1+m^2\beta^2)+c}{m\beta(2d+c)}$$

$$\left.-\frac{c(m^2\beta^2-3)+4d(m^2\beta^2-1)}{m^2\beta^2-1}\cos^{-1}\frac{d(1-m^2\beta^2)+c}{m\beta c}\right\}$$

and

$$D = \frac{c^3 \pi m d}{4h(c - h)}$$

Wing Drag for $m\beta = 1$

$$\frac{\pi S}{8m(t/c)^2} C_{D_\infty} = \frac{mc^{5/2}}{6h^{3/2}(c - h)^{3/2}} \left[(2d + c - h)^{3/2} \sqrt{ch} \right.$$

$$\left. + (2d + h)^{3/2} \sqrt{c^2 - ch} - (2d + c)^{3/2} \sqrt{ch - h^2} \right]$$

APPENDIX B

EVALUATION OF EQUATIONS (7) FOR TIP EFFECTS

For aspect-ratio limitations, see equations (6).

Section drag, $m\beta \leq 1$

$$\frac{c\pi\sqrt{1 - m^2\beta^2}}{4m(t/c)^2} c_{d_{tip}} = A + B + C$$

where A is evaluated in the region $\frac{md(1 + m\beta) - mc}{1 + m\beta} \leq y \leq md$ and is equal to

$$\frac{c^2}{4h(c - h)}\left[\frac{\sqrt{1 - m^2\beta^2}}{m}(y - md)\cosh^{-1}\frac{y + m(c - d)}{m\beta(md - y)} + c\cosh^{-1}\frac{(1 - m^2\beta^2)(y - md) + mc}{m^2c\beta}\right]$$

B is evaluated in the region $\frac{md(1 + m\beta) - m(c - h)}{1 + m\beta} \leq y \leq md$ and is equal to

$$\frac{-c^3}{4h(c - h)^2}\left[\frac{\sqrt{1 - m^2\beta^2}}{m}(y - md)\cosh^{-1}\frac{y + m(c - d - h)}{m\beta(md - y)} + (c - h)\cosh^{-1}\frac{(1 - m^2\beta^2)(y - md) + m(c - h)}{m^2(c - h)\beta}\right]$$

and C is evaluated in the region $\frac{md(1 + m\beta) - mh}{1 + m\beta} \leq y \leq md$ and is equal to

$$\frac{-c^3}{4h^2(c - h)}\left[\frac{\sqrt{1 - m^2\beta^2}}{m}(y - md)\cosh^{-1}\frac{y + m(h - d)}{m\beta(md - y)} + h\cosh^{-1}\frac{(1 - m^2\beta^2)(y - md) + mh}{m^2h\beta}\right]$$

Section drag, $m\beta > 1$

$$\frac{c\pi\sqrt{m^2\beta^2 - 1}}{4m(t/c)^2}c_{d_{tip}} = A + B + C$$

where A is evaluated in the region $\frac{md(1 + m\beta) - mc}{1 + m\beta} \leq y \leq md$ and is equal to

$$\frac{c^2}{4h(c - h)}\left[\frac{\sqrt{m^2\beta^2 - 1}}{m}(y - md)\cosh^{-1}\frac{y + m(c - d)}{m\beta(md - y)} + c\cos^{-1}\frac{(1 - m^2\beta^2)(y - md) + mc}{m^2c\beta}\right]$$

B is evaluated in the region $\frac{md(1 + m\beta) - m(c - h)}{1 + m\beta} \leq y \leq md$ and is equal to

$$\frac{-c^3}{4h(c - h)^2}\left[\frac{\sqrt{m^2\beta^2 - 1}}{m}(y - md)\cosh^{-1}\frac{y + m(c - d - h)}{m\beta(md - y)} + (c - h)\cos^{-1}\frac{(1 - m^2\beta^2)(y - md) + m(c - h}{m^2(c - h)\beta}\right.$$

and C is evaluated in the region $\frac{md(1 + m\beta) - mh}{1 + m\beta} \leq y \leq md$ and is equal to

$$\frac{-c^3}{4h^2(c - h)}\left[\frac{\sqrt{m^2\beta^2 - 1}}{m}(y - md)\ \cosh^{-1}\frac{y + m(h - d)}{m\beta(md - y)} + h\ \cos^{-1}\frac{(1 - m^2\beta^2)(y - md) + mh}{m^2h\beta}\right]$$

The increment in wing wave drag caused by the tip is identically equal to zero for all cases satisfying the aspect-ratio limitations.

REFERENCES

1. Puckett, A. E., and Stewart, H. J.: Aerodynamic Performance of Delta Wings at Supersonic Speeds. Jour. Aero. Sci., vol. 14, no. 10, Oct. 1947, pp. 567 – 578.

2. Margolis, Kenneth: Supersonic Wave Drag of Sweptback Tapered Wings at Zero Lift. NACA TN No. 1448, 1947.

3. Jones, Robert T.: Thin Oblique Airfoils at Supersonic Speed. NACA TN No. 1107, 1946.

4. Taylor, G. I., and Maccoll, J. W.: The Mechanics of Compressible Fluids. Two-Dimensional Flow at Supersonic Speeds. Vol III of Aerodynamic Theory, div. H, ch. IV, sec. 1, W. F. Durand, ed., Julius Springer (Berlin), 1935, p. 236.

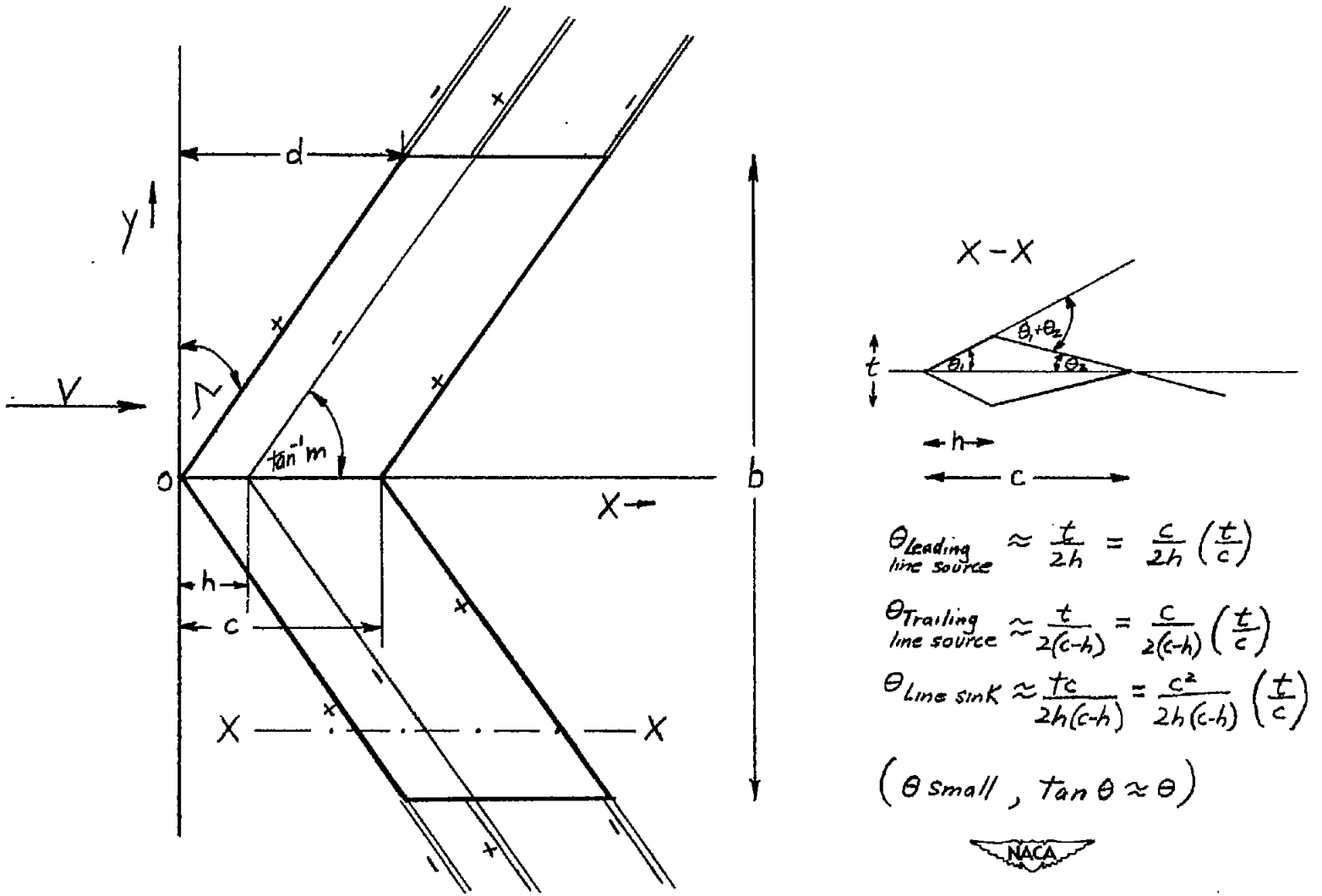

Figure 1.- Symbols, wedge angles, and distributions of sinks and sources for an untapered wing.

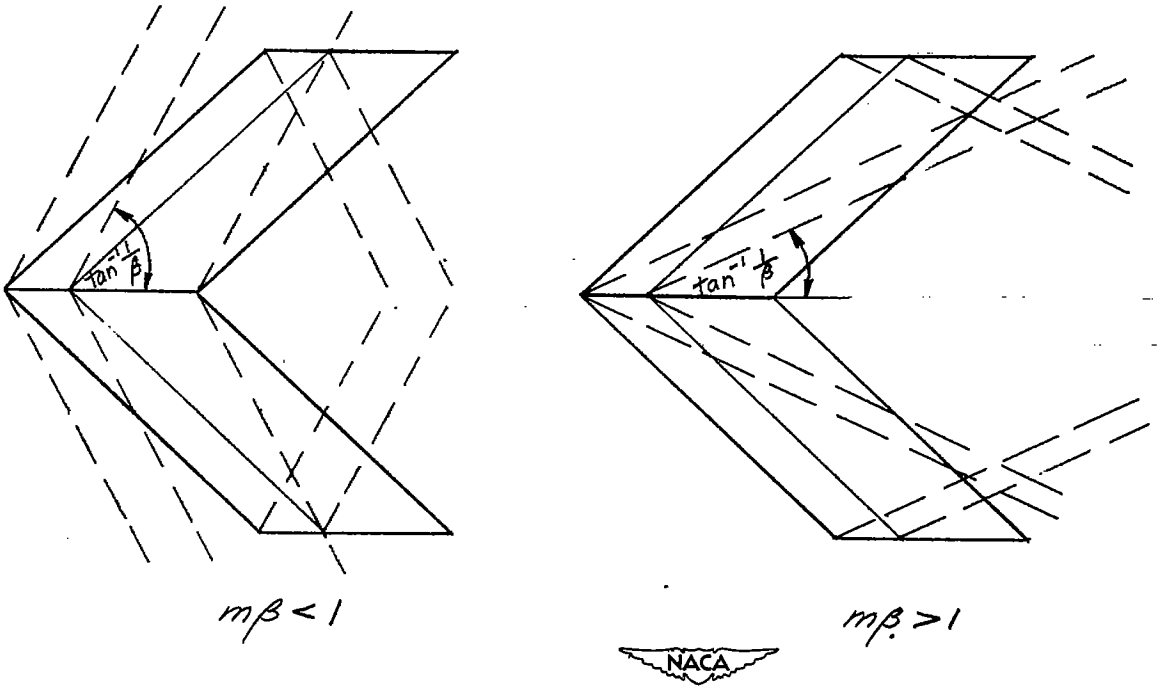

Figure 2.- Mach line configurations for untapered plan forms.

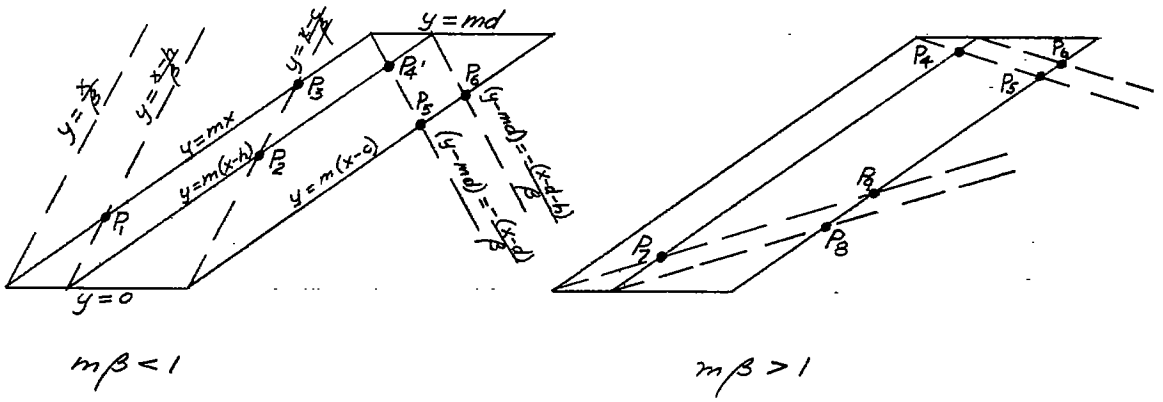

P	y-value	P	y-value	P	y-value
P_1	$\frac{mh}{1-m\beta}$	P_4	$\frac{md(1+m\beta)-mh}{1+m\beta}$	P_7	$\frac{mh}{m\beta-1}$
P_2	$\frac{m(c-h)}{1-m\beta}$	P_5	$\frac{md(1+m\beta)-mc}{1+m\beta}$	P_8	$\frac{m(c-h)}{m\beta-1}$
P_3	$\frac{mc}{1-m\beta}$	P_6	$\frac{md(1+m\beta)-m(c-h)}{1+m\beta}$	P_9	$\frac{mc}{m\beta-1}$

NACA

Figure 3.- Information pertinent to integration limits in equations (5) and (7).

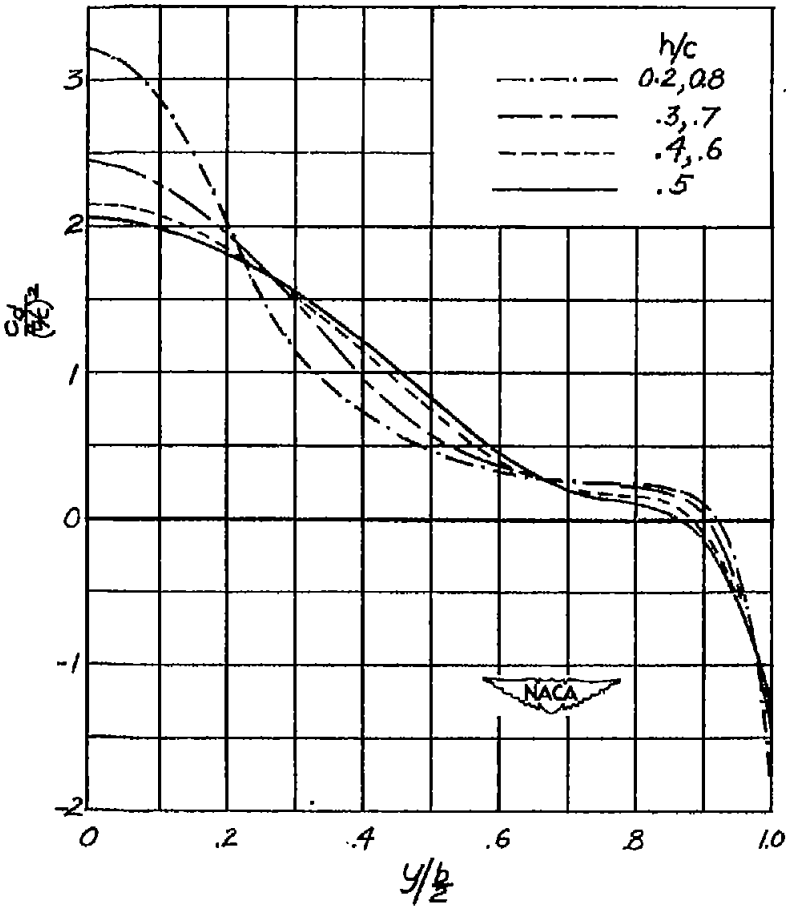

Figure 4.- Distributions of section wave drag for various maximum-thickness locations. Taper ratio, 1; Mach number, 1.414; aspect ratio, 2; sweepback angle, 60°.

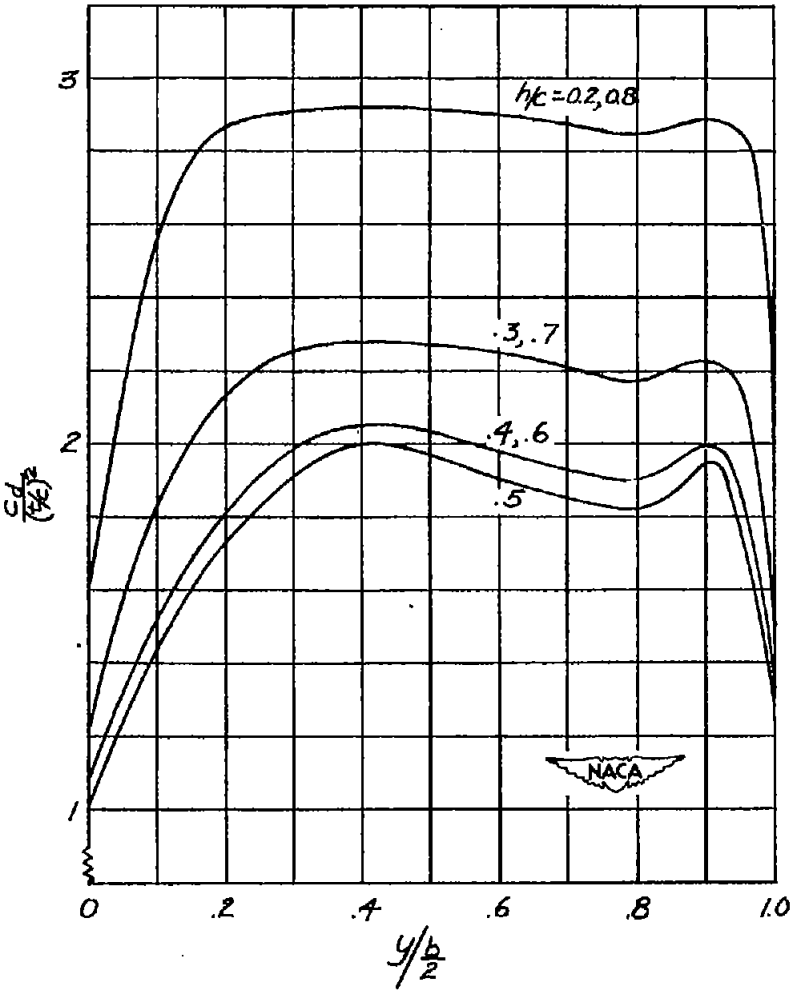

Figure 5.- Distributions of section wave drag for various maximum-thickness locations. Taper ratio, 1; Mach number, 3; aspect ratio, sweepback angle, 60°.

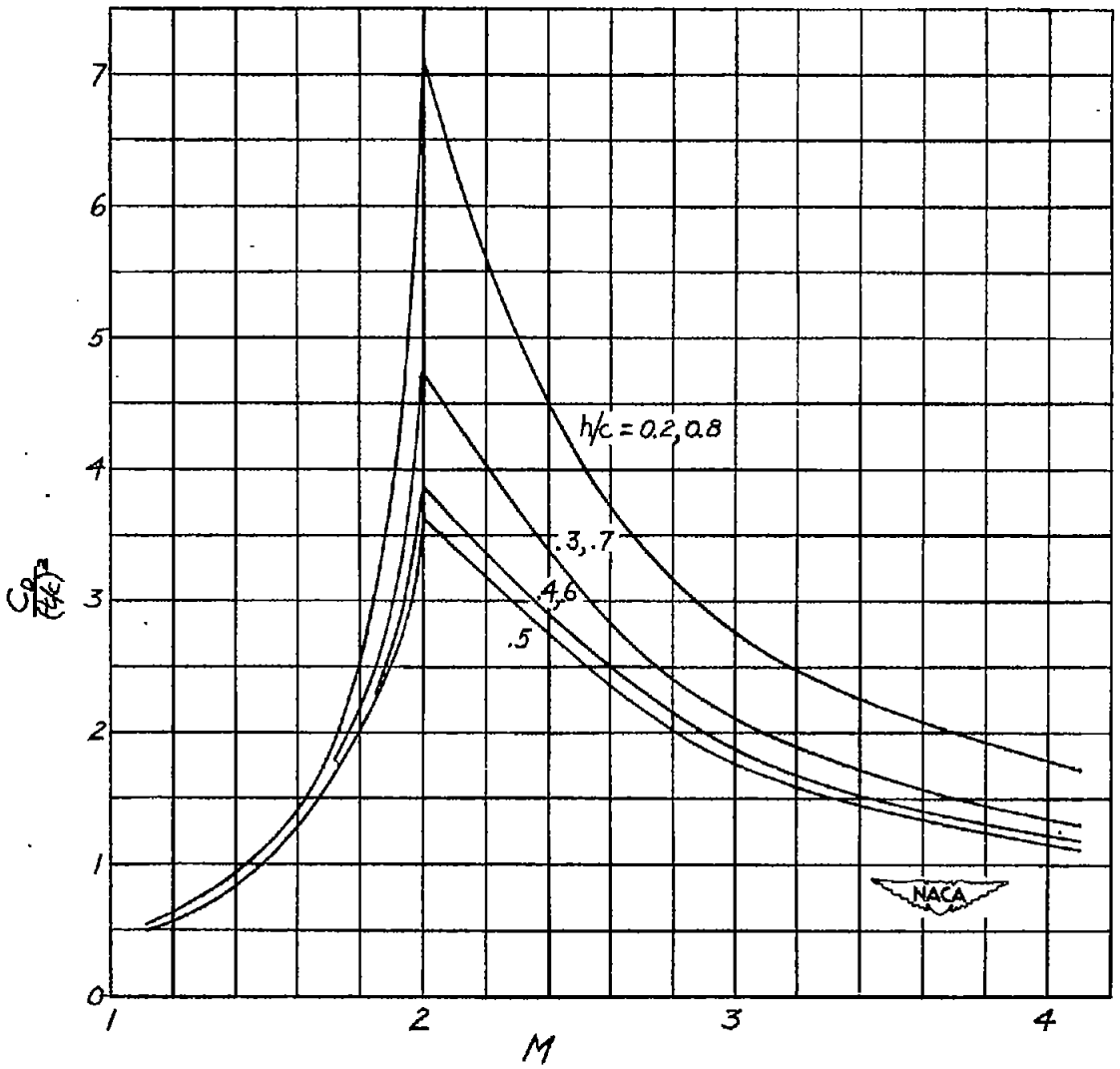

Figure 6.- Variation of wing wave-drag coefficient with Mach number for various maximum-thickness locations. Aspect ratio, 2; taper ratio, 1; sweepback angle, 60°.

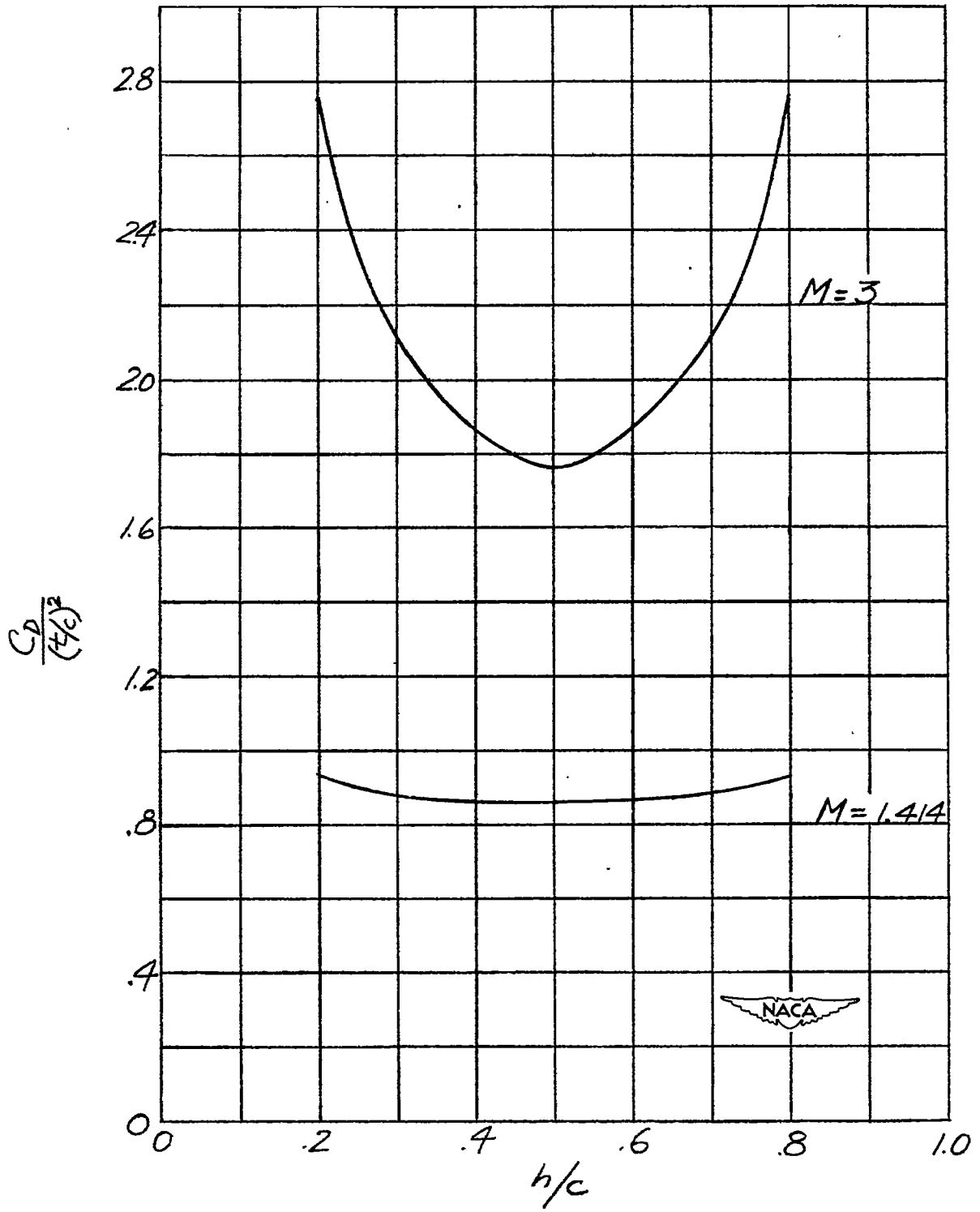

Figure 7.- Variation of wing wave-drag coefficient with maximum-thickness location. Taper ratio, 1; aspect ratio, 2; sweepback angle, 60°.

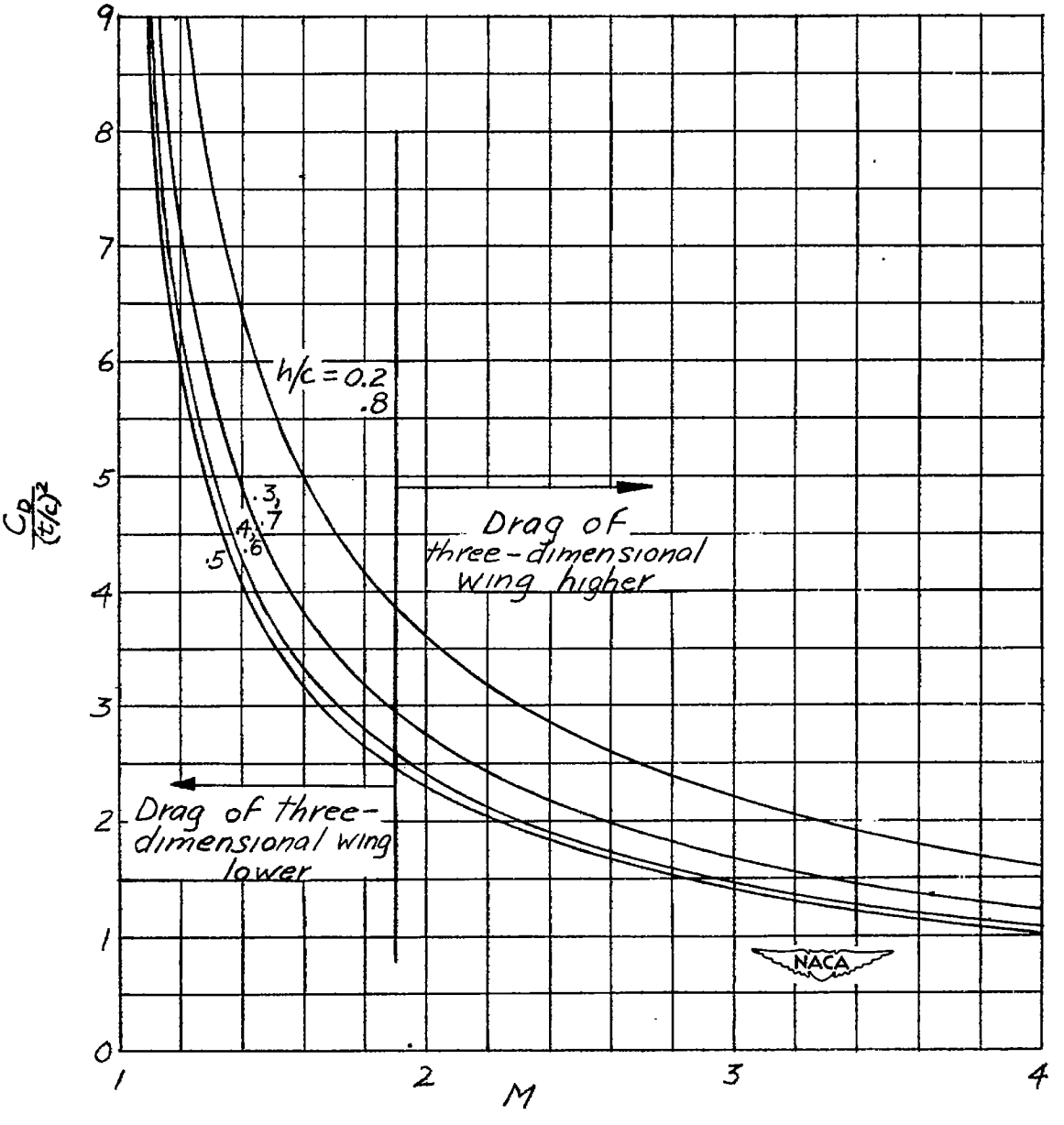

Figure 8.- Two-dimensional variation of wing wave-drag coefficient with Mach number for various maximum-thickness locations and comparison with three-dimensional result for untapered wing. Aspect ratio, 2; sweepback angle, 60°.